Supplementary Files

Controlled Release of Hydrogen by Implantation of Magnesium Induces P53-mediated Tumor Cells Apoptosis

Rui Zan[a, b#], Hao Wang[c#], Weijie Cai[d#], Jiahua Ni[a*], Bérengère J. C. Luthringer-Feyerabend[b], Wenhui Wang[a], Hongzhou Peng[a], Weiping Ji[d], Jun Yan[e], Jiazeng Xia[c*], Yang Song[a*], Xiaonong Zhang[a,f*]

[a] State Key Laboratory of Metal Matrix Composites, School of Materials Science and Engineering, Shanghai Jiao Tong University, Shanghai 200240, China

[b] Institute of Metallic Biomaterials, Department of Biological Characterisation, Helmholtz-Zentrum Geesthacht (HZG), Geesthacht 21502, Germany

[c] Department of General Surgery and Translational Medicine Center, Wuxi No.2 People's Hospital, Affiliated Wuxi Clinical College of Nantong University, Jiangsu 214002, China

[d] Orthopaedic Department, Shanghai Jiao Tong University Affiliated Sixth People's Hospital, Shanghai 200233, China

[e] Department of General Surgery, Shanghai Jiao Tong University Affiliated Sixth People's Hospital, Shanghai 200233, China

[f] Suzhou Origin Medical Technology Co. Ltd., Suzhou 215513, China

[#] **Authors contributed equally to this work.**

Corresponding authors: nijiahua2012@gmail.com (Dr. J. Ni);

jiazengxia@yahoo.com (Dr. J. Xia);

nanosurface@sjtu.edu.cn (Dr. Y. Song);

xnzhang@sjtu.edu.cn (Dr. X. Zhang).

Materials and methods

The H_2 evolution in cell culture. H_2 collection devices were used in cell culture experiments with an atmosphere of 5% CO_2 at 37 °C. After 48 h in the cell incubator, the volume of released H_2 in different groups was quantitively measured by the weight loss of Mg sheets. Before weighting, the corroded samples were rinsed in an aqueous solution containing 180 g/L CrO_3, and 10 g/L $AgNO_3$. A loss of 1.083 mg of Mg produced 1mL H_2 [1]. Besides, the surface morphology and roughness of the Mg sheets after immersion in PBS were observed using scanning electron microscopy (FEI, USA) and confocal laser scanning microscopy (CLSM, Zeiss, German). In the meantime, the concentration of dissolved H_2 in culture medium was measured by a dissolved hydrogen analyzer.

Detection of intracellular ROS content. The intracellular ROS level was tested by exposing tumor and normal cells to H_2 for 48 h. Then, cells were collected by trypsin digestion and stained by 2,7-Dichlorodi-hydrofluorescein diacetate (DCFH-DA) ROS-sensitive probe (YEASEN, China). The intracellular ROS content was quantitively analyzed by a flow cytometer after washed twice by culture medium without FBS.

Detection of oxidative stress and antioxidant enzymes. The contents of MDA and SOD in tumor cells were measured by using kits purchased from Jiancheng Biotechnology Research Institute (Nanjing, China). The operation procedure was according to the manufacturer's protocol.

Detection of ATP. The concentration of ATP in tumor cells was tested by the Luminescence ATP Detection Assay System (PerkinElmer, USA). The HCT116 cells

were seeded in the H_2-producing device and treated with different amounts of H_2. After 48 h, the cells were transferred to a 96-well plate, added with 100 μL ATP detection agent and then shaken for 3 min. The luminescence of cells was measured by a multimode microplate reader (Tecan & Spark, Switzerland).

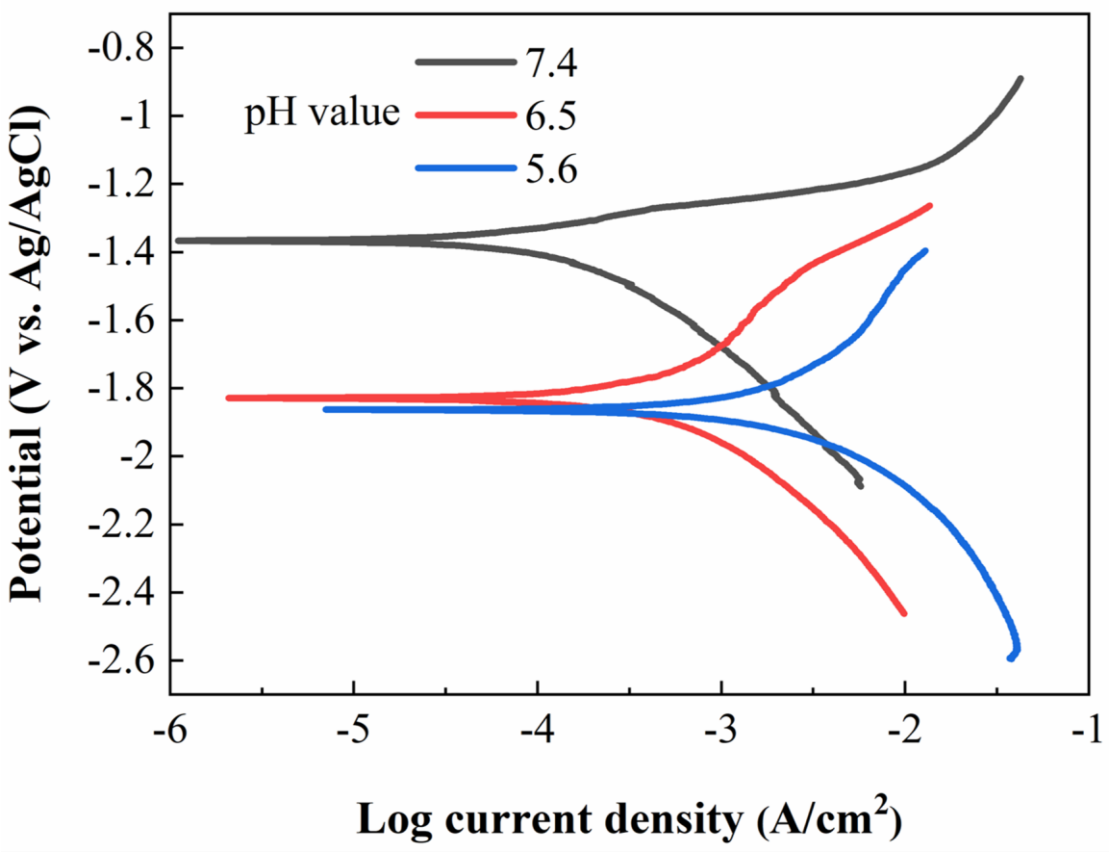

Figure S1 Typical cathodic potentiodynamic polarization curves for Mg sheet in different pH values of PBS solution.

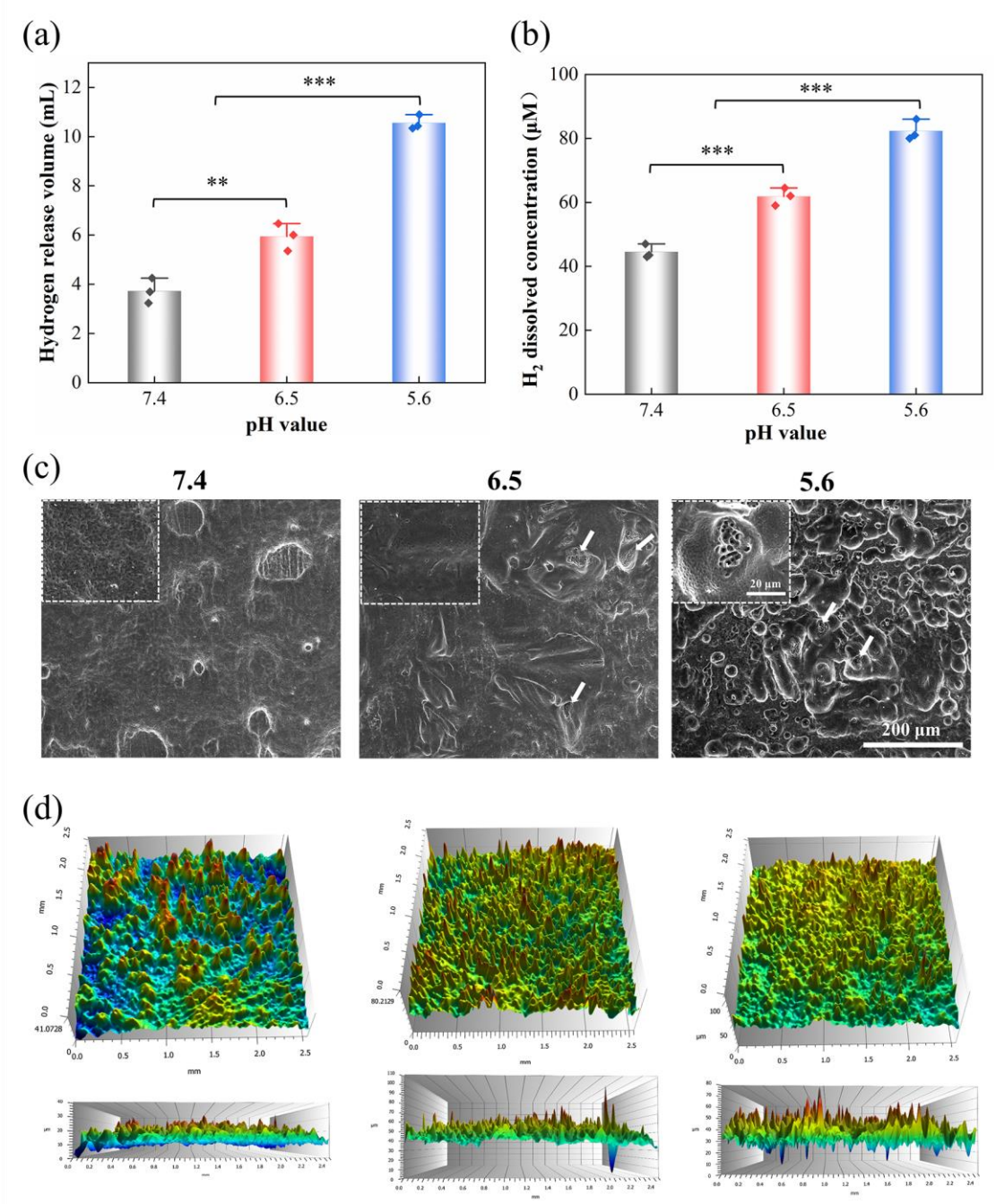

Figure S2 (a) The release volume of H_2 when Mg samples immersed in PBS solution with different pH values for 48 h in a cell incubator. (b) The corresponding concentration of dissolved H_2 in culture medium in the upper transwell chamber. The SEM (c) and CLSM (d) images of Mg samples immersed in PBS solution with different pH values for 48 h in cell incubator after corrosion layer removing.

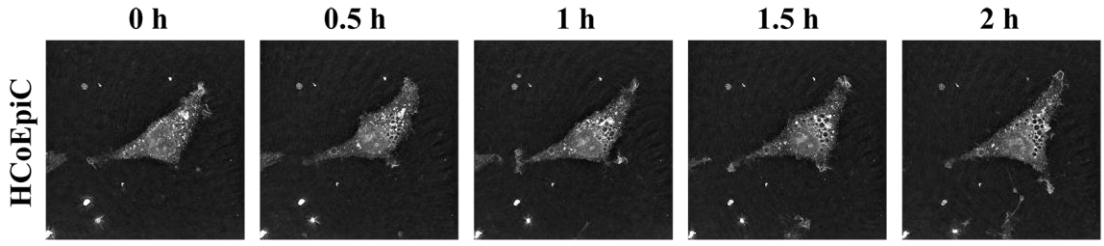

Figure S3 A series of morphology images of HCT116 cells from a live cell imaging microscope.

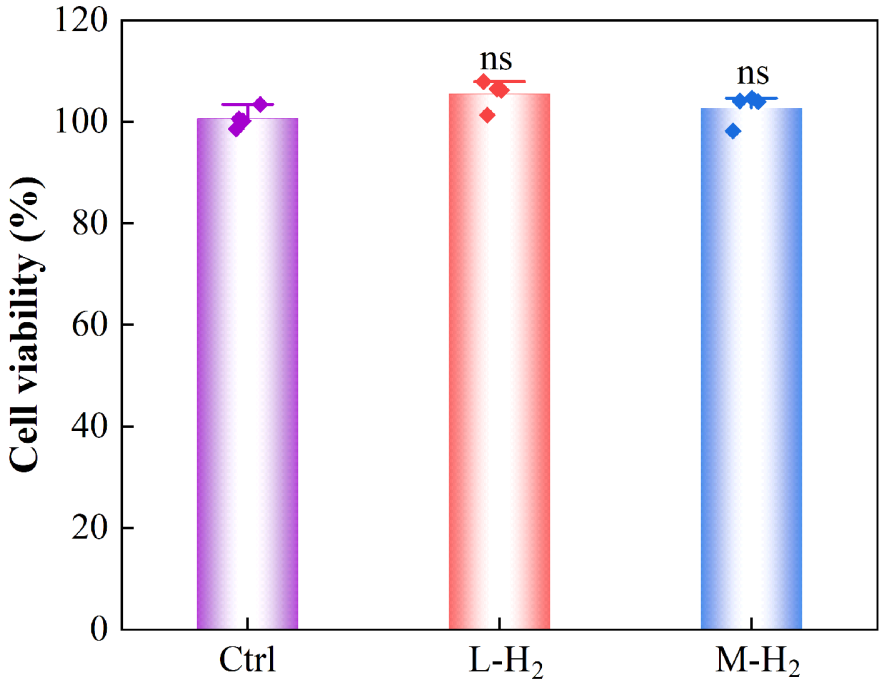

Figure S4 The cell viability of human colonic epithelial cells (HCoEpiC) with different treatments for 72 h.

The differences of hydrogen to the viability of tumor and normal tissue cells may be explained by the selective scavenging activity of H_2 against redundant cytotoxic ROS in tumor cells, but not affect the role of essential ROS metabolites in normal cells, as shown in Fig. S5. Besides, the released H_2 reduced the oxidative stress in tumor cells by alleviating the level of oxidative protein malondialdehyde (MDA) and increasing antioxidant enzyme superoxide dismutase (SOD) activity (Fig. S6).

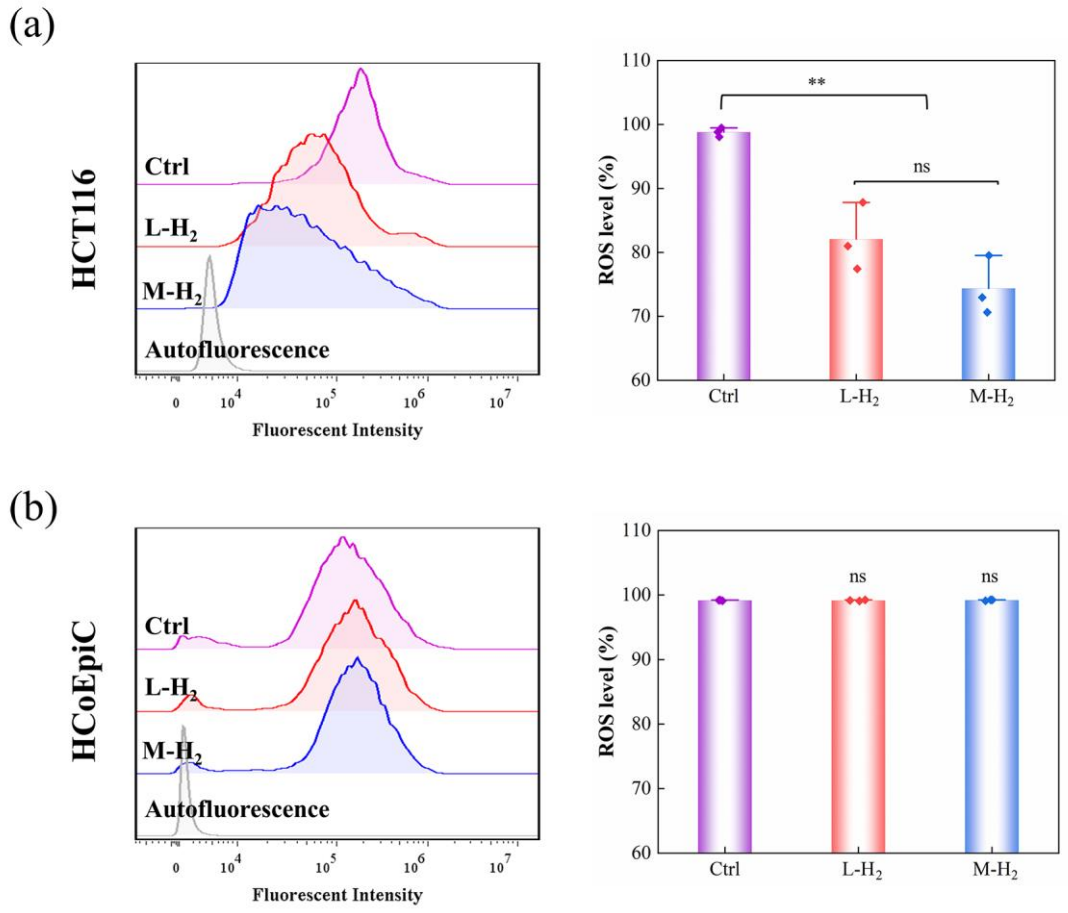

Figure S5 The intracellular reactive oxygen species (ROS) level and the relatively quantitive analysis in HCT116 (a) and HCoEpiC (b) cells with different treatments for 48 h.

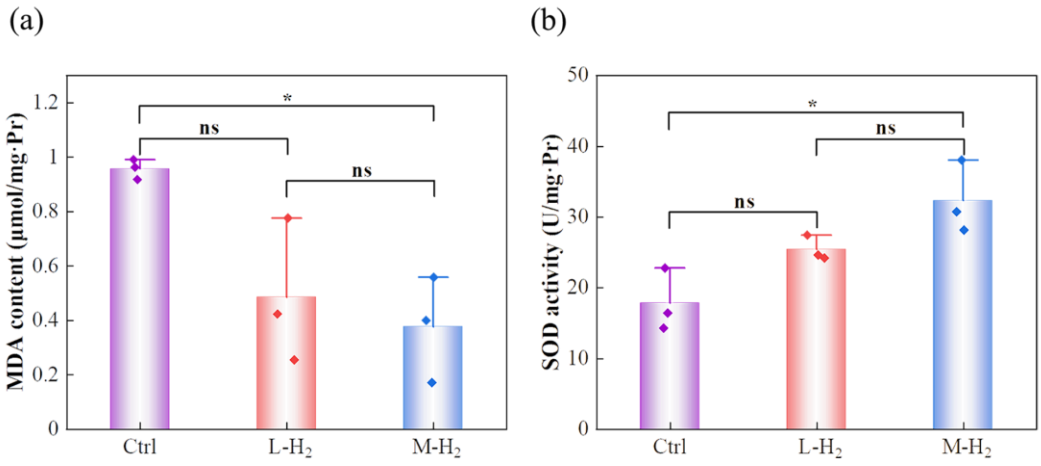

Figure S6 The MDA level (a) and SOD activity in HCT116 cells with different treatments for 48 h.

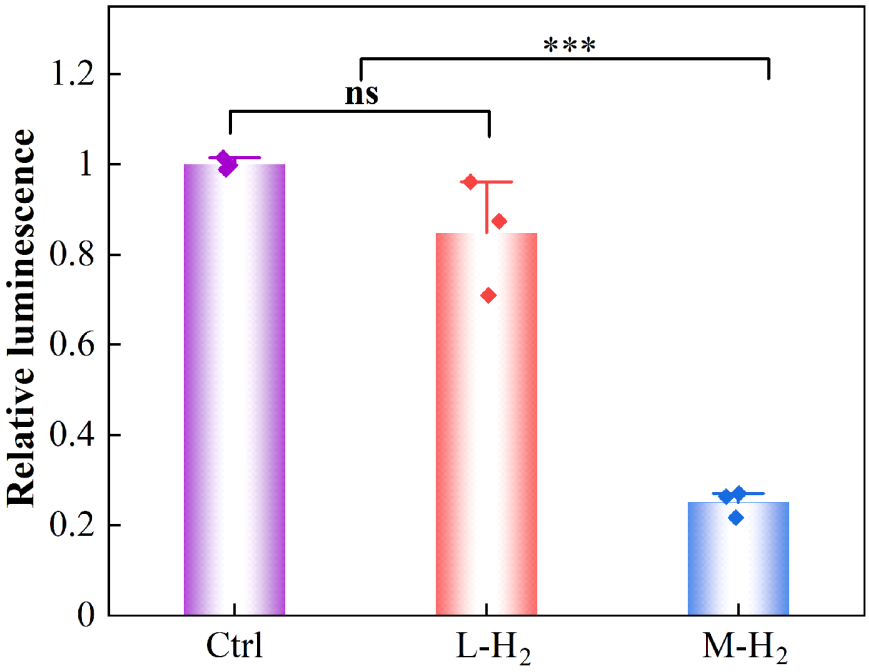

Figure S7 The ATP content in HCT116 cells with different treatments by luminescence ATP Detection Assay.

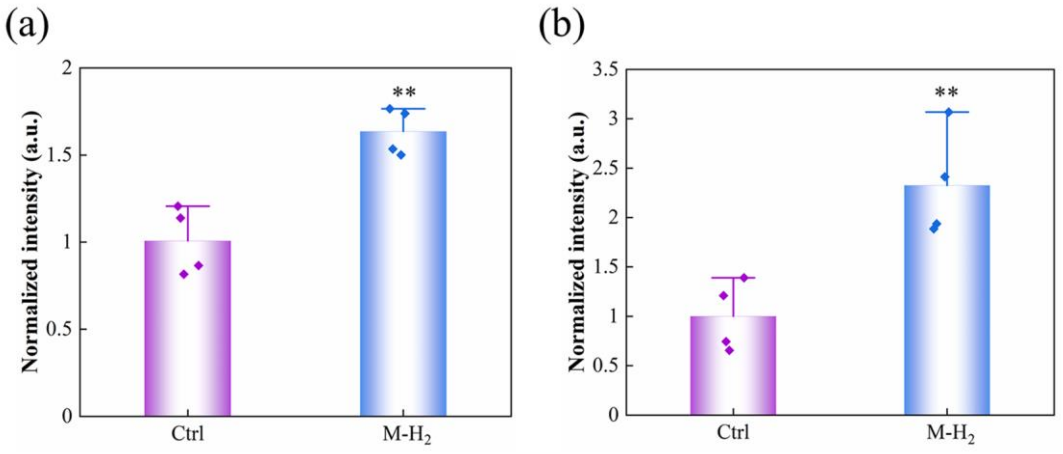

Figure S8 The quantification of cytochrome C (a) and caspase 3 (b) fluorescent intensity from the confocal fluorescence images of HCT116 cells in the Ctrl and M-H_2 groups.

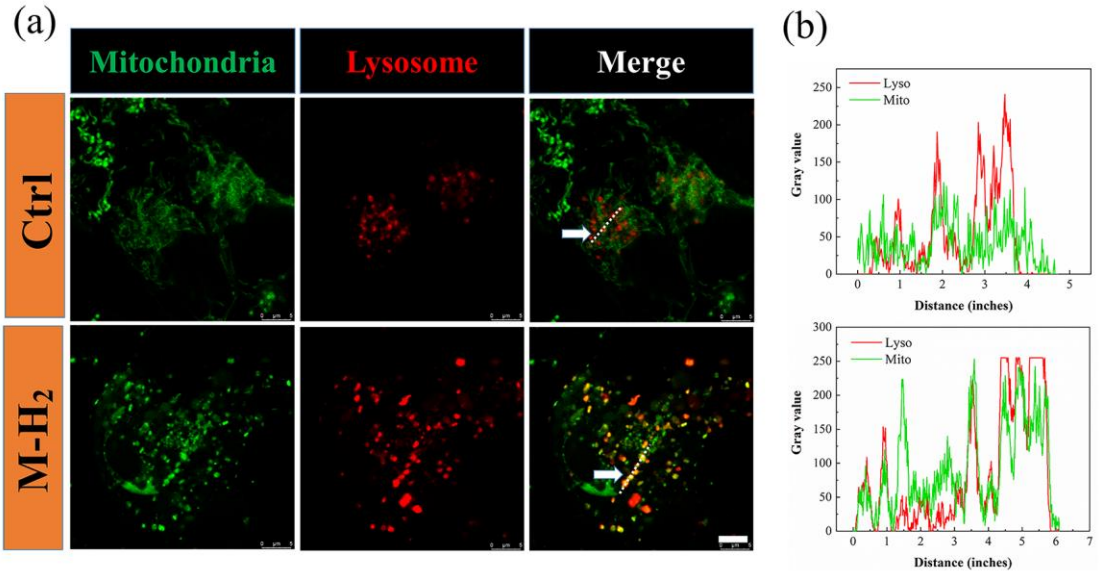

Figure S9 (a) CLSM images to detect the colocalization of mitochondria and lysosome and the scale bar is 5 μm. (b) Colocalization analysis of selected area with a white dotted line.

The volumetric ratio of hydrogen dissolved in tumors to the total hydrogen produced by Mg (η) is estimated from the Mg plate (exposed surface at 24 mm^2/mL, for 720 min) *in vitro* immersion test. The η is calculated as follows:

$n(H_2\text{-}d)=C_sV_s = 145.5 \times 0.01=1.455$ μM

where $n(H_2\text{-}d)$ is the mole of the dissolved hydrogen; C_s is the concentration of dissolved H_2 in PBS solution at 720 min and V_s is the volume of the PBS solution.

$n(H_2\text{-}r)= \frac{PV}{RT}= \frac{101.325\times0.00026}{8.314\times310.15}=10.217$ μM (under standard atmosphere pressure)

Where $n(H_2\text{-}r)$ is the mole of the released hydrogen; P is atmosphere pressure; V is the volume of released hydrogen for 720 min; T is temperature and R is the ideal gas constant.

$\eta=\frac{n(H_2-d)}{n(H_2-r)} \times \%=1.455/10.217 \times \%=14.24\%$

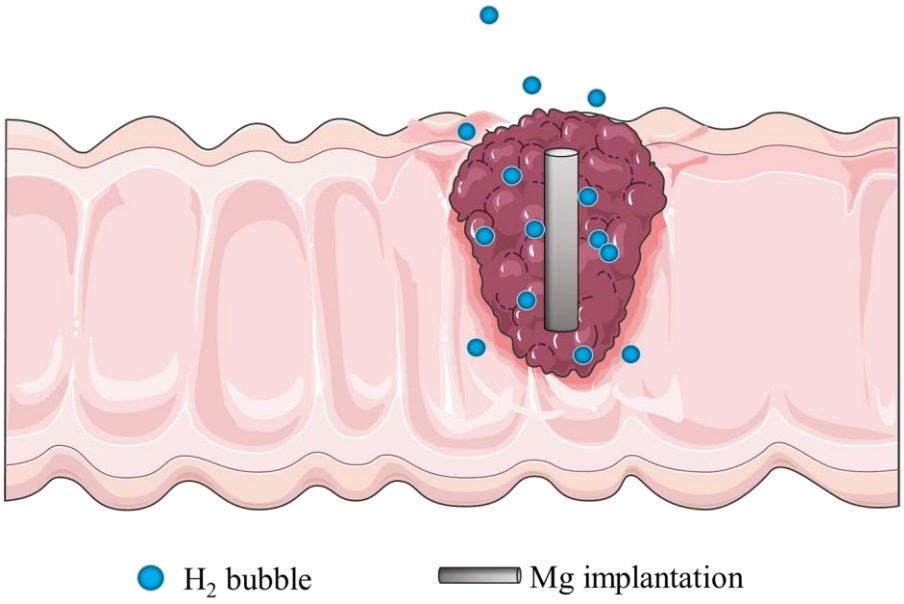

Figure S10 The schematic illustration Mg implantation into colorectal carcinoma to releases H_2 and part of H_2 dissolving in tumors.

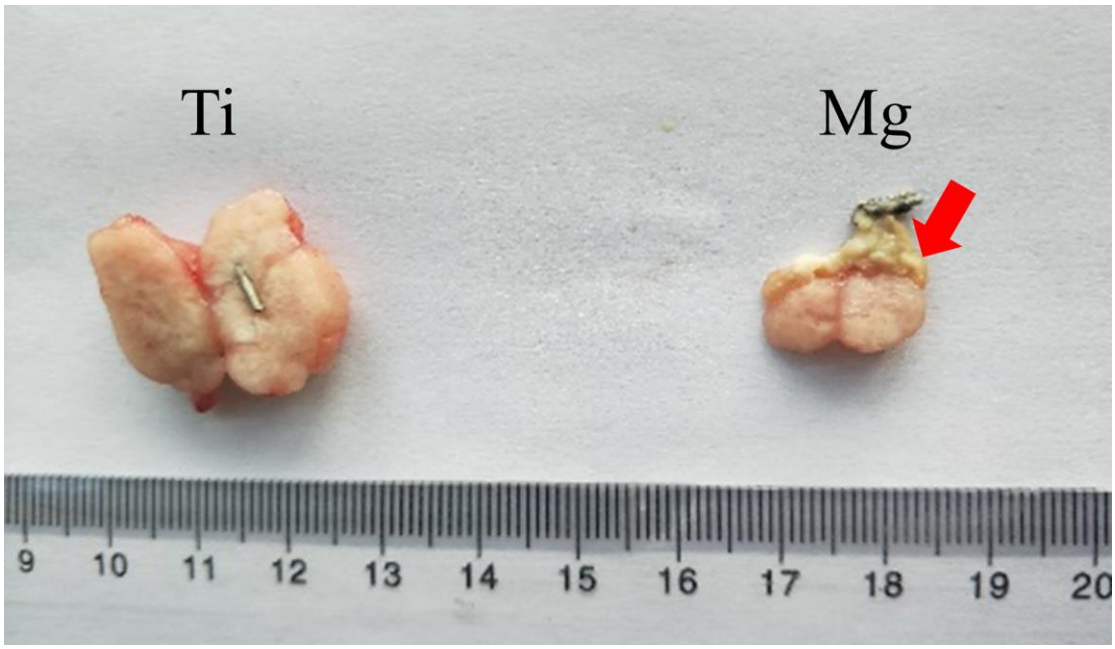

Figure S11 The photograph of tumor tissues inserted by Ti (left) and Mg (right) wires.

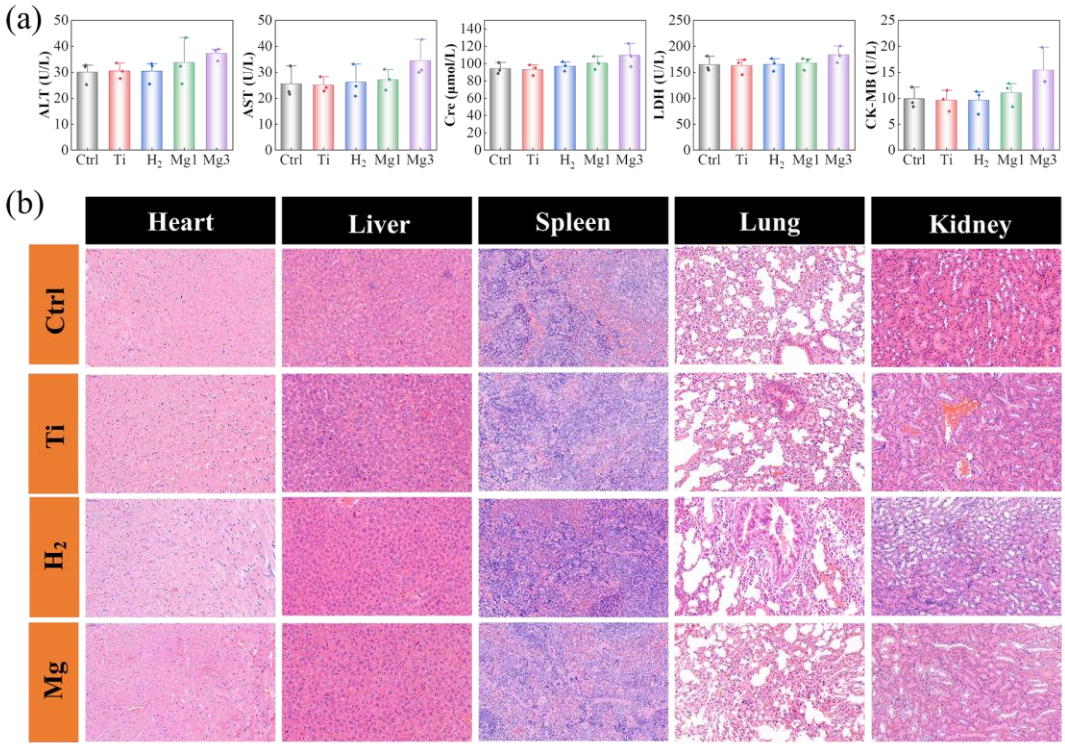

Figure S12 (a) Haematology data of the tumor-bearing mice with different treatments on the 24th day. (b) H&E staining of the major organs of mice on day 24th.

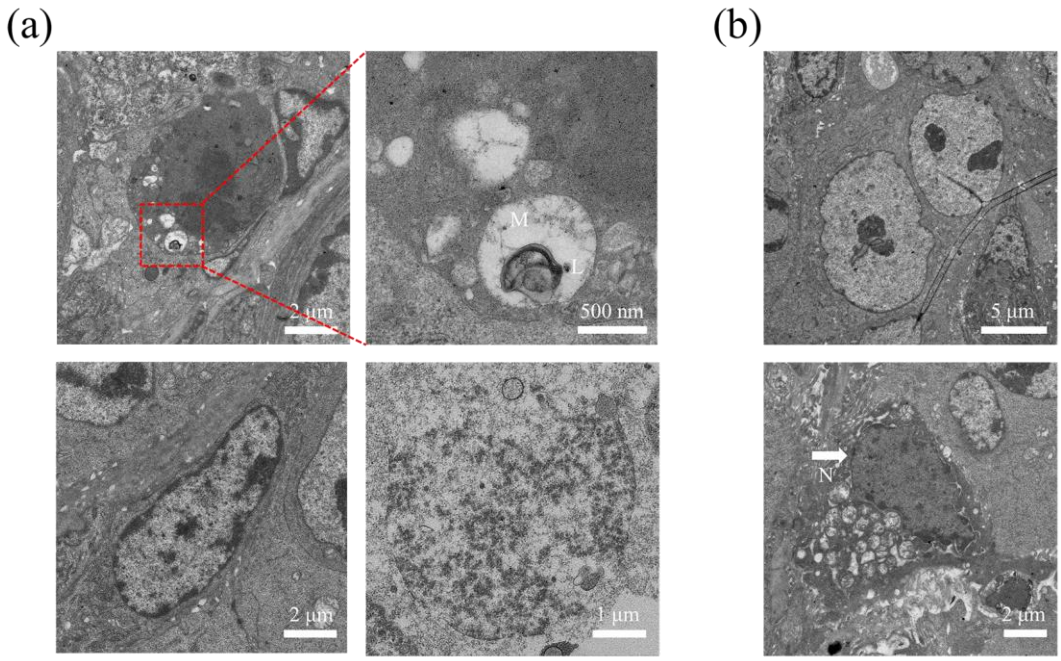

Figure S13 (a) Typical apoptotic features of HCT116 cells in tumor tissues were observed, including swollen and vacuolated mitochondria (top), aggregation of nucleus chromatin on the edge and expansion of nuclear membrane (down left) and apoptotic body (down right); (b) some immune cells were found near Mg wires, including foreign body multinucleated giant cells (FBGCs) (top) and neutrophils cells (down). M, L and N indicate mitochondria, lysosome and neutrophils cells, respectively.

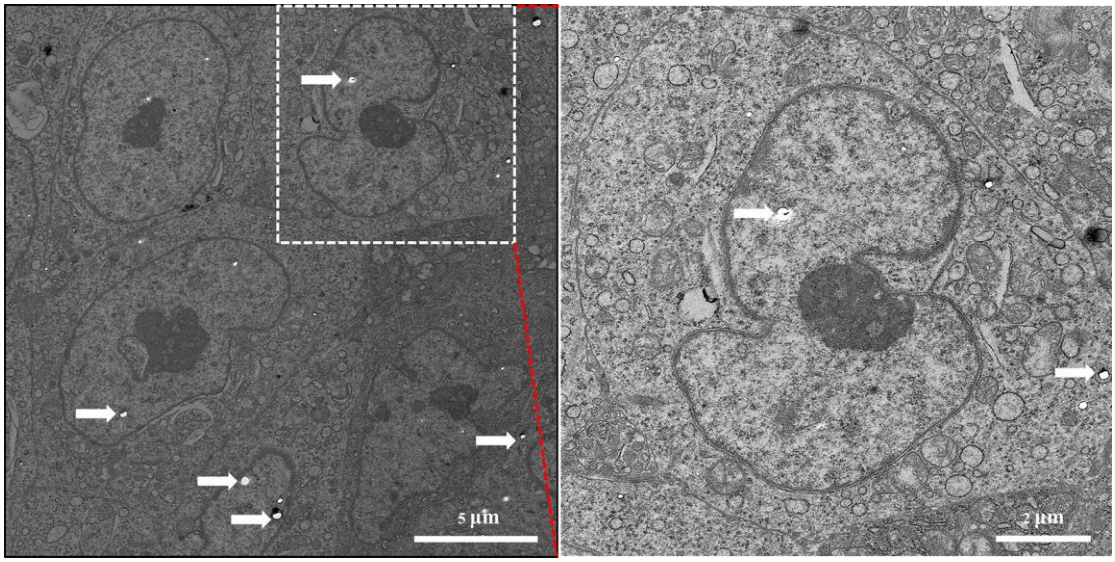

Figure S14 TEM photos of the tumor tissues in the distant region of Mg wire.

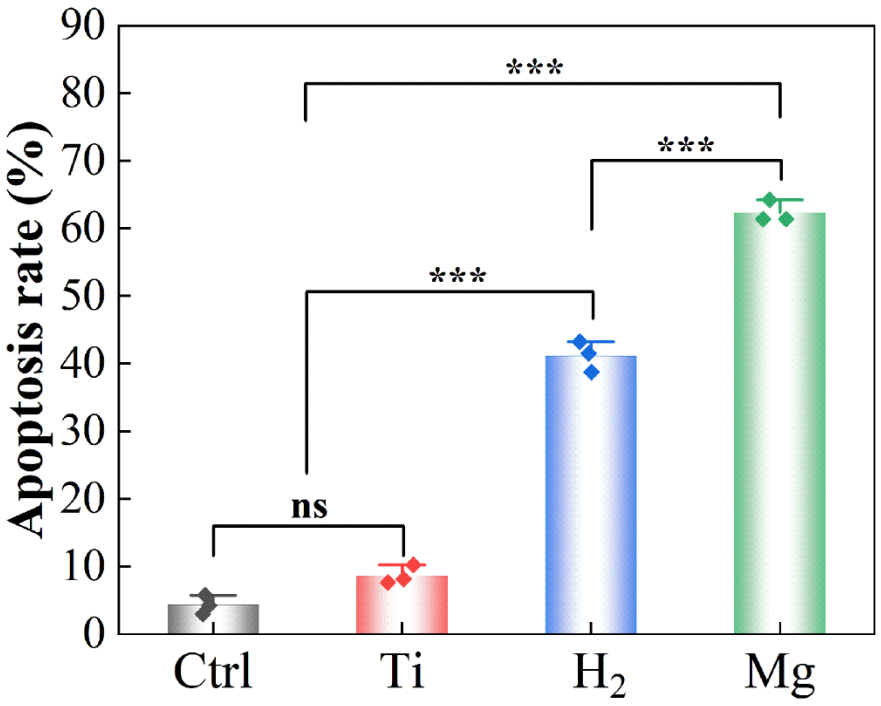

Figure S15 Relative apoptosis rate of the tumor tissue is quantified for each group of mice by TUNEL assay.

Table S1 E_{corr} and I_{corr} values of Mg in PBS solution with pH values of 5.6, 6.5 and 7.4.

pH value	E_{corr} (V. vs Ag/AgCl)	I_{corr} (mA cm^{-2})
7.4	-1.57 ± 0.11	$6.10 \pm 0.19 \times 10^{-5}$
6.5	-1.86 ± 0.02	$3.27 \pm 0.39 \times 10^{-4}$
5.6	-1.91 ± 0.13	$1.54 \pm 0.28 \times 10^{-3}$

Table S2 Abbreviations and full names of genes are labeled in the circular visualization of the results of gene-annotation enrichment analysis.

IL21R	interleukin 21 receptor	CSF3	colony stimulating factor 3
HLA-DPA1	Major histocompatibility complex, class II, DP alpha 1	MPL	MPL proto-oncogene, thrombopoietin receptor
FAS	Fas cell surface death receptor	CNTFR	ciliary neurotrophic factor receptor
HLA-DOA	major histocompatibility complex, class II, DO alpha	PIK3CG	phosphatidylinositol-4,5-bisphosphate 3-kinase catalytic subunit gamma
SOCS1	suppressor of cytokine signaling 1	GHR	growth hormone receptor
SPRY1	sprouty RTK signaling antagonist 1	IL1A	interleukin 1 alpha
HLA-DPB1	major histocompatibility complex, class II, DR beta 1	HLA-DPA1	major histocompatibility complex, class II, DP alpha 1
CRLF2	cytokine receptor like factor 2	OCLN	occludin
CLDN3	claudin 3	CLDN23	claudin 23
MADCAM1	mucosal vascular addressin cell adhesion molecule 1	JUN	Jun proto-oncogene, AP-1 transcription factor subunit
CLDN1	claudin 1	JAM2	junctional adhesion molecule 2
CD274	CD274 molecule	PTGS2	prostaglandin-endoperoxide synthase 2
FCGR2C	Fc fragment of IgG receptor IIc (gene/pseudogene)	NCF2	neutrophil cytosolic factor 2
CTF1	cardiotrophin 1	ULBP1	UL16 binding protein 1
ULBP2	UL16 binding protein 2	SH2D1B	SH2 domain containing 1B
HLA-DRB1	major histocompatibility complex, class II, DR beta 1	HSPA5	heat shock protein family A (Hsp70) member 5
GADD45B	growth arrest and DNA damage inducible beta	HSPA6	heat shock protein family A (Hsp70) member 6
SESN2	sestrin 2	SERPINE1	serpin family E member 1
CCNG2	cyclin G2	LTA	lymphotoxin alpha
CDKN1A	cyclin dependent kinase inhibitor 1A	LAMP3	lysosomal associated membrane protein 3

CD68	CD68 molecule	DNASE2	deoxyribonuclease 2, lysosomal
NEU1	neuraminidase 1	RAET1L	retinoic acid early transcript 1L
TNFRSF10C	TNF receptor superfamily member 10c	TNFRSF10B	TNF receptor superfamily member 10b

References

[1] Z. Shi, A. Atrens, An innovative specimen configuration for the study of Mg corrosion, Corros. Sci. 53(1) (2011) 226-246.